Paper No. 1.11

SECOND INTERNATIONAL CONFERENCE ON PERFORMANCE-BASED DESIGN IN EARTHQUAKE GEOTECHNICAL ENGINEERING

May 28-30, 2012 - TAORMINA (ITALY)

DEVELOPMENT OF A MODIFIED ELASTOPLASTICITY MODEL FOR SAND

Panagiota TASIOPOULOU [1], Nikos GEROLYMOS[2]

ABSTRACT

The key prerequisite to performance based design of geotechnical structures is the reliable estimation of the induced displacements. Thus, the need for advanced yet practical constitutive modeling of soil behavior continuously becomes more profound and demanding. This paper presents a new simple effective stress model for drained and undrained behavior of sand under monotonic and cyclic loading conditions, with emphasis on liquefaction. The model is formulated in the framework of classical elastoplasticity, and combines features of: (a) the bounding surface plasticity, (b) the critical state concept, and (c) a hardening evolution law and unloading-reloading rule of the modified Bouc-Wen type. The predictive capabilities of the model are demonstrated through simulations of loading tests in p-q space.

Keywords: Constitutive model of sand, Bouc-Wen model, plasticity, critical state concept, liquefaction, static and cyclic loading

INTRODUCTION

Performance based analysis is increasingly gaining ground in daily practice against conventional pseudostatic analysis. The necessity of developing economically efficient solutions without jeopardizing safety, is the main reason for this drastic change in the way we you used to design our structures.

However, the effectiveness of a performance based design approach strongly hinges on the ability of the utilized numerical tool to realistically calculate the soil and structural displacements for a wide range of loading paths and initial conditions. Apparently, the constitutive modeling of soil behavior plays a decisive role on this. The behavioral diversity of sand for different loading (drained /undrained, monotonic/cyclic), initial stress and fabric conditions, renders its modeling a difficult and challenging task. The suitability of the used constitutive model is evaluated by its capability to capture the trends across all these conditions without recalibration of its parameters for each specific case, but also by its simplicity. Too many parameters might increase the versatility of the model at the risk, however, of losing its physical meaning.

In the last three decades, many constitutive models for sand have been proposed, each with varying degree of accuracy and applicability. The most promising ones are plasticity-based and incorporate the effective stress and critical state concepts (e.g.: Ishihara and Towhata, 1980; Cubrinovski and Ishihara,

[1] PhD Candidate, School of Civil Engineering, National Technical University, Athens, e-mail: ptasiopoulou@gmail.com

[2] Lecturer, School of Civil Engineering, National Technical University, Athens, e-mail: gerolymos@gmail.com

2000; Dafalias and Mazari, 2004; Park and Byrne, 2004; Boulanger et all., 2011). In this paper, a brief mathematical description of a new constitutive model for sand under development is presented.

The model, which is an extension of the BWGG constitutive law (Gerolymos, 2002; Gerolymos and Gazetas, 2005) in 3-dimensional stress space, combines features of the bounding surface plasticity and critical state concept. Having the BWGG genes in its DNA, the proposed model can be consistent with almost any pair of shear modulus and damping curves of the literature, while at the same time the corresponding experimentally observed hysteretic soil behavior is realistically reproduced. At this stage of development the Drucker-Prager failure envelope is used as bounding surface, but modifications can be easily implemented to account for Lode angle dependency. The combined influence of density and confining stress on the response is efficiently taken into account through the critical state approach.

The ability of the model to realistically reproduce complex patterns of monotonic and cyclic behavior such us densification and associated strength hardening in drained cyclic loading, loss of strength and cyclic mobility in undrained monotonic and cyclic loading, respectively, without readjustment of its parameters, is highlighted through a series of numerical examples in p-q loading space.

CONSTITUTIVE EQUATIONS

Review of classical elastoplacity

Within the framework of deformation theory of classical elastoplasticity, the incremental total deformation, $d\boldsymbol{\varepsilon}$ is decomposed into the elastic and plastic components $d\boldsymbol{\varepsilon}^e$ and $d\boldsymbol{\varepsilon}^p$ by a simple superposition:

$$d\boldsymbol{\varepsilon} = d\boldsymbol{\varepsilon}^e + d\boldsymbol{\varepsilon}^p \tag{1}$$

The plastic strain increment is obtained from the flow rule:

$$d\boldsymbol{\varepsilon}^p = \langle L \rangle \frac{\partial g}{\partial \boldsymbol{\sigma}} \tag{2}$$

implying normality to the plastic potential function g. L is a positive scalar of proportionality designated as the loading index.

Substituting Eq. (2) into Eq. (1) and applying elasticity theory, the following stress-strain relationship is obtained:

$$d\boldsymbol{\sigma} = \boldsymbol{E}^e \left(d\boldsymbol{\varepsilon} - \langle L \rangle \frac{\partial g}{\partial \boldsymbol{\sigma}} \right) \tag{3}$$

For a perfectly plastic material, the yield surface is fixed in stress space, and therefore plastic deformation occurs only when the stress path moves on the yield surface. Thus, the loading condition at failure is postulated by the following consistency equation:

$$df = 0 \Rightarrow \left(\frac{\partial f}{\partial \boldsymbol{\sigma}} \right)^{\mathrm{T}} d\boldsymbol{\sigma} = 0 \tag{4}$$

Combining Eqs (3) and (4), and after some algebra, the stress-strain relationship is reformulated into:

$$d\boldsymbol{\sigma} = \boldsymbol{E}^{ep} d\boldsymbol{\varepsilon} \tag{5}$$

in which $\boldsymbol{E}^{ep}$ is the elasto-plastic matrix, given by:

$$\boldsymbol{E}^{ep} = \boldsymbol{E}^{e}\left[\boldsymbol{I} - \boldsymbol{\Phi}_{g}\left(\boldsymbol{\Phi}_{f}^{T}\boldsymbol{E}^{e}\boldsymbol{\Phi}_{g}\right)^{-1}\boldsymbol{\Phi}_{f}^{T}\boldsymbol{E}^{e}\right] \tag{6}$$

in which $\boldsymbol{\Phi}_f$ and $\boldsymbol{\Phi}_g$ account for the failure surface and plastic flow rule, respectively:

$$\boldsymbol{\Phi}_{f} = \frac{\partial f}{\partial \boldsymbol{\sigma}} \quad , \quad \boldsymbol{\Phi}_{g} = \frac{\partial g}{\partial \boldsymbol{\sigma}} \tag{7}$$

Modified elastoplacity

Hardening and Unloading-Reloading laws

Hardening and hysteretic behavior is introduced by inserting the matrices $\boldsymbol{H}$ and $\boldsymbol{\eta}$ into Eq. (6):

$$\boldsymbol{E}_{h}^{ep} = \boldsymbol{E}^{e}\left(\boldsymbol{I} - \boldsymbol{BH}\right)\boldsymbol{\eta} \tag{8}$$

The terms in matrix $\boldsymbol{H}$ are functions of the dimensionless hardening parameter ζ, which is of the Bouc-Wen type (Gerolymos and Gazetas, 2005), and $\boldsymbol{\eta}$ (Gerolymos and Gazetas, 2005; Drosos et al., 2012) accounts for stiffness degradation by modifying the shape and size of the hysteretic loops according to the amplitude of the deviatoric strain ε_q . For the sake of simplicity, $\boldsymbol{\eta}$ is set equal to the unity matrix in all subsequent numerical examples. Finally, $\boldsymbol{B}$ is the abbreviation of the right-hand side term inside the parentheses of Eq. (6):

$$B = \boldsymbol{\Phi}_{g}\left(\boldsymbol{\Phi}_{f}^{T}\boldsymbol{E}^{e}\boldsymbol{\Phi}_{g}\right)^{-1}\boldsymbol{\Phi}_{f}^{T}\boldsymbol{E}^{e} \tag{9}$$

Elastic Moduli

The terms in matrix $\boldsymbol{E}^{e}$ includes the shear and bulk moduli which are expressed as functions of the mean effective stress p, according to:

$$G = A_{o}\,p_{\alpha}\left(\frac{p}{p_{\alpha}}\right)^{m} \quad , \quad K = \frac{2\left(1+v\right)}{3\left(1-2v\right)}G \tag{10}$$

in which, A_o is a dimensionless material parameter, v is the Poisson's ratio, p_a is the atmospheric pressure, and m is a dimensionless parameter determining the rate of variation of G and K with p.

Formulation in p-q space

Yield Function

At the current stage of development, the model incorporates the Drucker-Prager failure envelope as the bounding surface:

$$f = q - M_{s}\,p = 0 \tag{11}$$

In which, M_s is the ultimate strength line in q-p space.

Eq. (11) implies the following consistency condition at failure:

$$f = 0 \Leftrightarrow \frac{q}{M_s p} = 1 \tag{12}$$

Following Eq. (12), the hardening parameter, ζ, is defined as:

$$\zeta = \left| \frac{q}{M_s p} \right|^n \tag{13}$$

In which n is an exponential parameter which "controls" the distance of the current stress state from the failure line (Gerolymos and Gazetas, 2005). The hardening parameter, ζ, is bounded, strictly obtaining values within the range [-1 1]. At reversal points, ζ is transformed to ζ_α , according to:

$$\zeta_a = \left| \frac{\zeta - \zeta_{max}}{2} \right|^n \tag{14}$$

in which ζ_{max} is the maximum value of ζ at the most previous pivot point.

Flow rule

The stress-dilatancy relationship, adopted by the model, is based on Rowe's dilatancy theory (Rowe 1962). The ratio of the plastic volumetric strain increment, $d\varepsilon_p^p$, over the plastic deviatoric strain increment, $d\varepsilon_q^p$ depends on the distance of the current stress ration, $q / p = \zeta M_s$ from the phase transformation line, M_{pt}, as follows:

$$\frac{d\varepsilon_p{}^p}{\left| d\varepsilon_q{}^p \right|} = \left(M_{pt} - \zeta M_s \right) \tag{15}$$

Combining Eq. (15) with Eq. (2) and using the definition of ε_q^p in p-q space, the following expressions for $d\varepsilon_q^p$ and $d\varepsilon_p^p$ are obtained:

$$d\varepsilon_q{}^p = 3\langle L \rangle \tag{16}$$

and:

$$d\varepsilon_p{}^p = 3\langle L \rangle \left(M_{pt} - \zeta M_s \right) \tag{17}$$

Eqs (16) and (17), which imply that a non-associative flow rule is finally used, determine the formation of $\boldsymbol{\Phi}_g$ according to:

$$\boldsymbol{\Phi}_g = \begin{bmatrix} \frac{\partial g}{\partial p} \\ \frac{\partial g}{\partial q} \end{bmatrix} = \begin{bmatrix} 3\left(M_{pt} - \zeta M_s\right) \\ 3 \end{bmatrix} \tag{18}$$

Critical state concept

The essence of the critical state concept is that no change in volume occurs when the current stress state reaches the critical state, while the shear deformation continuously increases. In order to achieve this kind of performance upon critical state, both the phase transformation line, M_{pt} and the ultimate strength line, M_s should "move" in p-q space converging to the critical state line, M_{cs} and producing zero plastic volumetric change ($M_{pt} = M_s = M_{cs}$). The evolution of the ultimate strength line is expressed as a function of the plastic deviatoric strain:

$$M_s = M_{cs} + \left[M_{sp} + \left(M_{so} - M_{sp}\right) e^{-c_1 \left|\varepsilon_q{}^p\right|} - M_{cs} \right] e^{-c_2 \left|\varepsilon_p{}^p\right|} \tag{19}$$

where M_{so} is an initial value of the ultimate strength, and M_{sp} is a maximum value that can be potentially reached depending on the model parameters c_1 and c_2.
The phase transformation line evolves according to following expression:

$$M_{pt} = M_{cs} + \left(M_{pto} - M_{cs}\right) e^{-c_3 \left|\varepsilon_{pc}{}^p\right|} \qquad d\varepsilon_{pc}^p = \lambda \tag{20}$$

in which M_{pto} is the initial value of M_{pt} , c_3 is a model parameter and $de^p{}_{pc}$ is equal to $de_p^{\,p}$ for monotonic loading and $<de_p^{\,p}>$ for cyclic loading.

MODEL PERFORMANCE

Simulations of drained and undrained behavior of sand under monotonic and cyclic loading have been performed in p-q space (Figures 1-6). Regarding the monotonic loading, four different relative densities were examined. Specifically for the monotonic undrained case (Figures 1-3), the evolution of phase transformation and ultimate strength lines are illustrated in Figure 3 as a function of deviatoric strain, in order to better demonstrate that both lines reach the critical state line at large strains. Moreover, it is worth noting that for loose sands the phase transformation line is initially located above the ultimate strength line in p-q space and vice versa for denser sands. This is attributed to the more contractive behavior which leads them directly to the critical state with no phase transformation (Yoshimine and Ishihara, 1998). The opposite behavior is observed for denser sand which first crosses the phase transformation line (contractive response) before they "move" towards the critical state (dilative response).

The set of model parameters, shown in Table 1, is common for all simulations with two exceptions: i) for demonstrative purposes, n = 1.5 in cyclic drained simulation, and ii) the exponential parameter, c_2 , which shifts the M_s line from peak state (M_{sp}) towards critical state (M_{cs}), is zero in cyclic undrained simulation. The latter exception is due to the fact that as the stress path reaches the apex and the confining stress decreases, the ultimate strength line increases (Ishihara and Towhata, 1980).

Table 1. Model parameters

		Monotonic Loading (Drained & Undrained)				*Drained cyclic loading*	*Unrained cyclic loading*
		Very loose sand	Loose sand	Medium sand	Dense sand	Medium sand	Dense sand
Elasticity	A_o	250	250	250	250	250	250
	m	0.6	0.6	0.6	0.6	0.6	0.6
	v	0.2	0.2	0.2	0.2	0.2	0.2
Ultimate strength	M_{so}	1	1	1	1	1	1
	M_{sp}	1.2	1.3	1.4	1.8	1.4	1.8
	c_1	40	40	40	40	40	40
	c_2	40	40	40	40	40	0
Phase transformation	M_{pto}	1.22	1.14	0.9	0.5	0.9	0.5
	c_3	40	40	40	40	40	40
Critical state	M_{cs}	1.2	1.2	1.2	1.2	1.2	1.2
Hardening	n	0.7	0.7	0.7	0.7	1.5	0.7

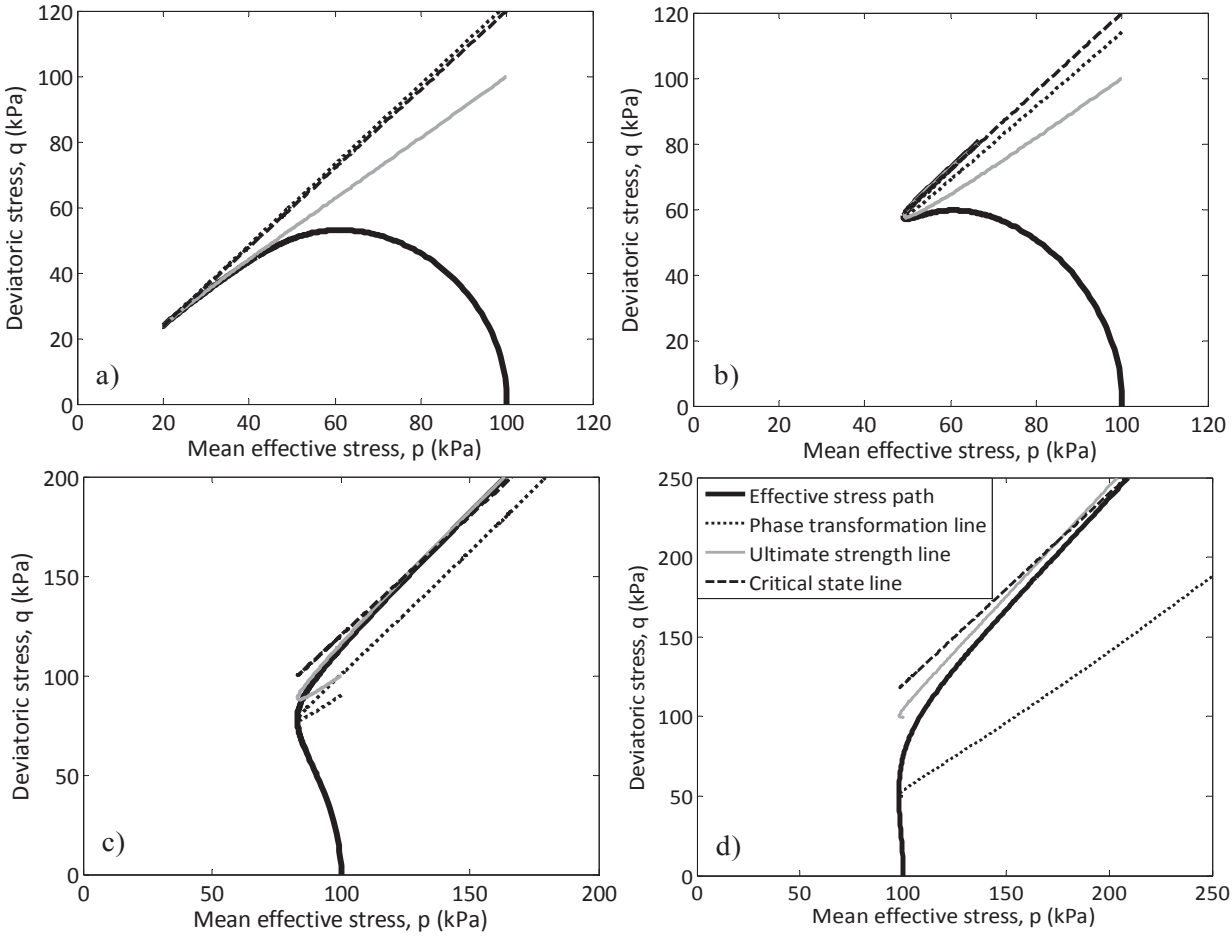

Figure 1. Simulation of monotonic undrained behavior of sand: a) very loose, b) loose, c) medium and d) dense sand.

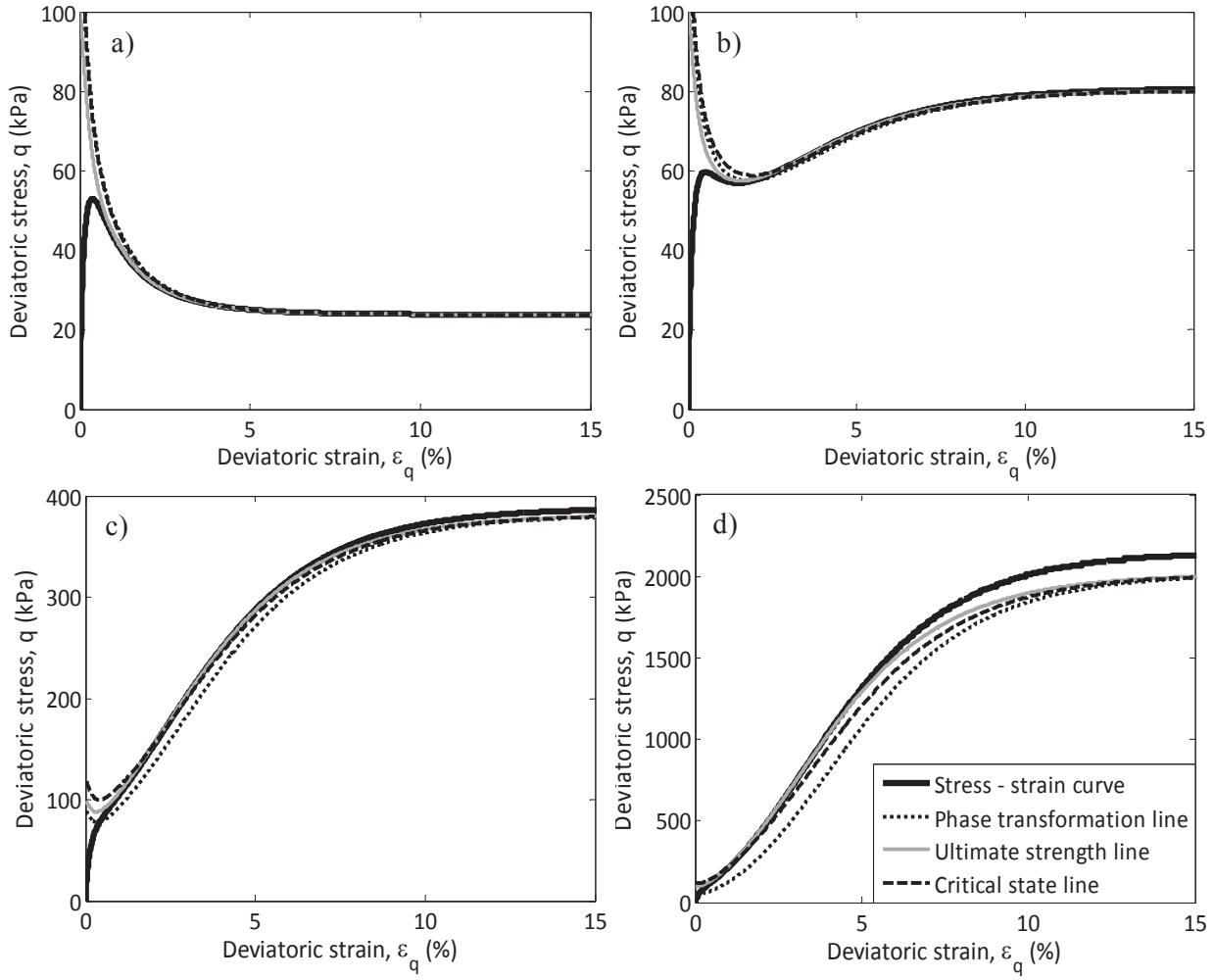

Figure 2. Simulation of monotonic undrained behavior of sand: a) very loose, b) loose, c) medium and d) dense sand.

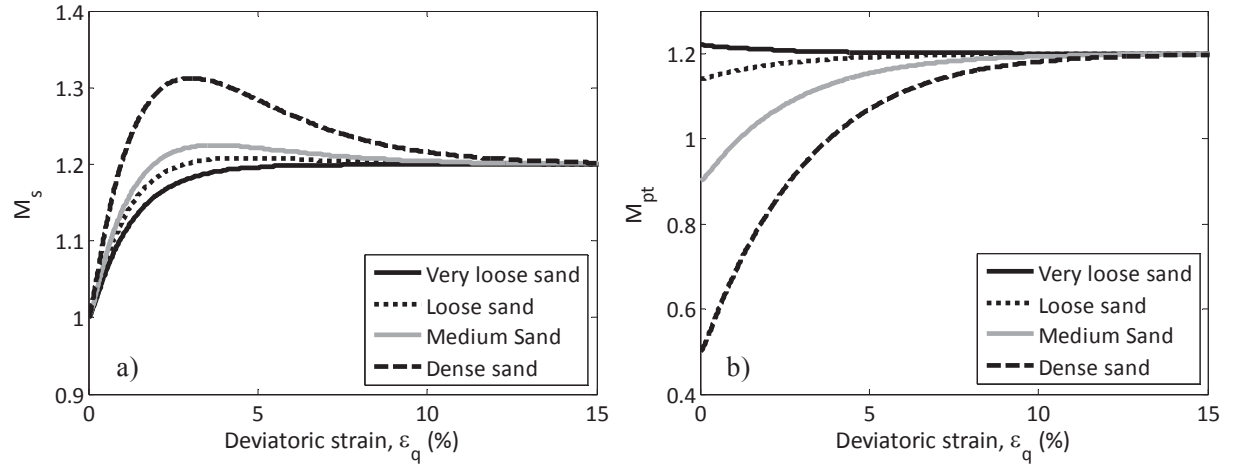

Figure 3. Evolution of ultimate strength, M_s and phase transformation lines, M_{pt} during simulation of monotonic undrained loading.

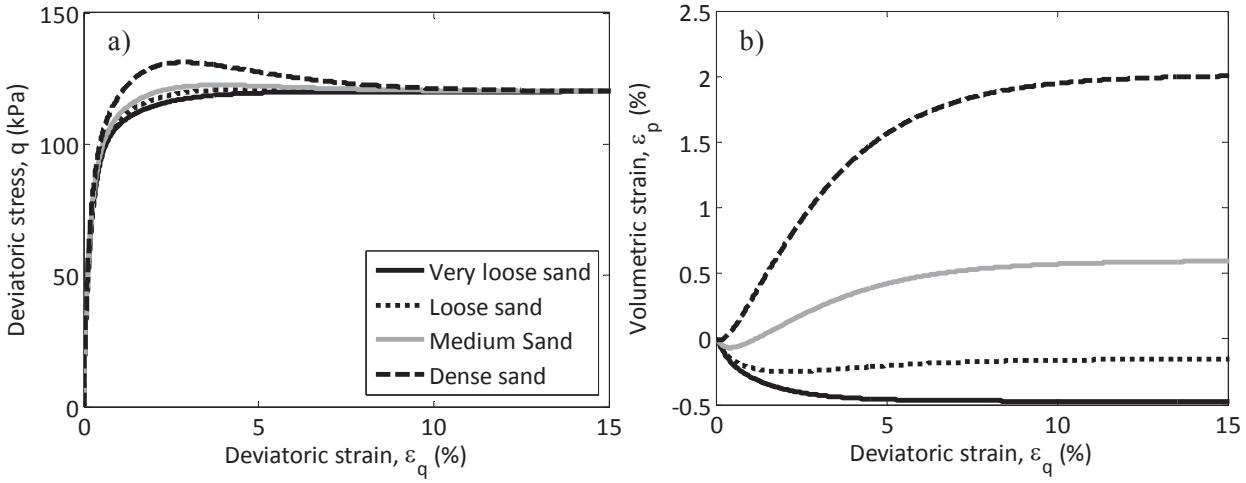

Figure 4. Simulation of monotonic drained behavior of sand.

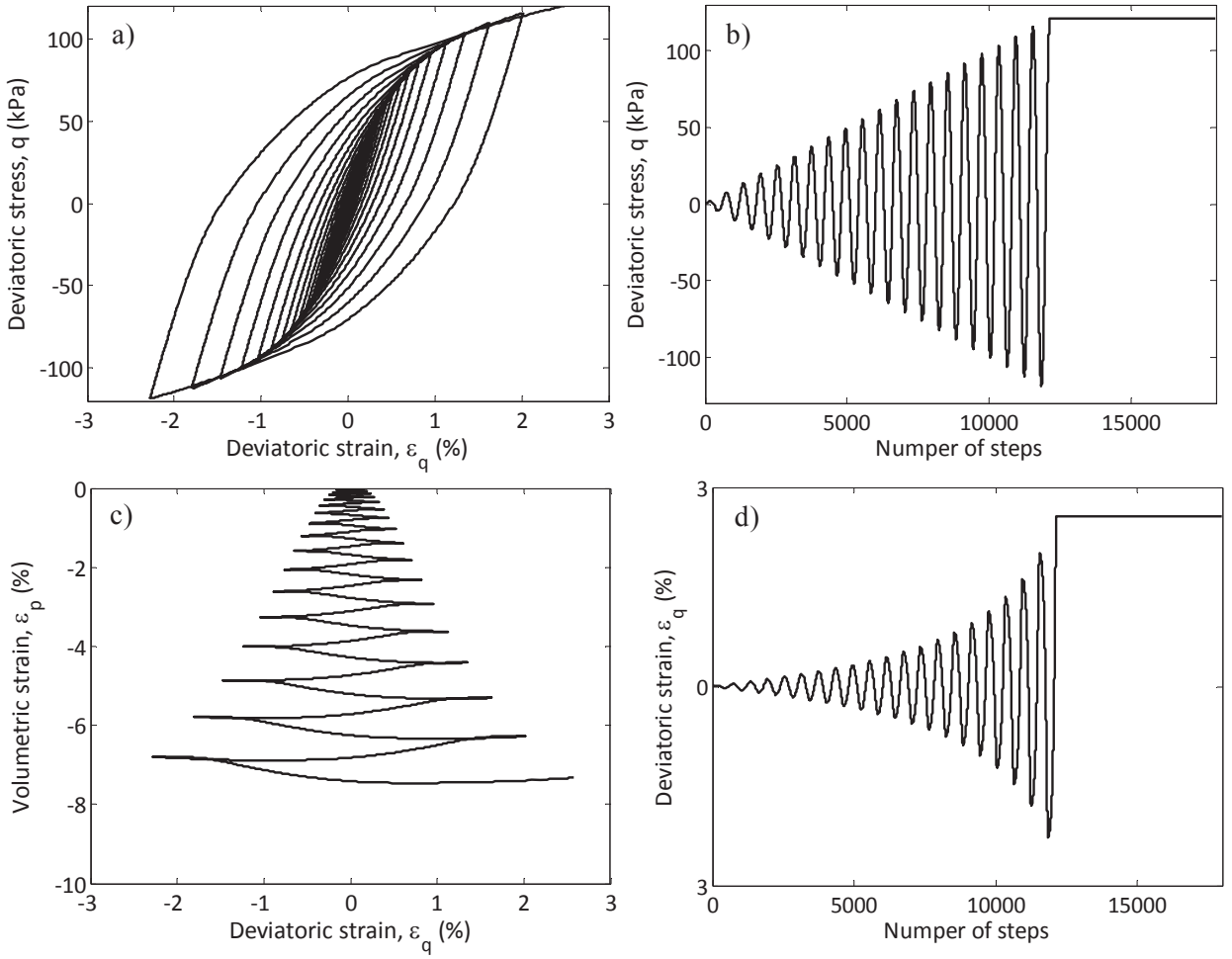

Figure 5. Simulation of cyclic drained behavior of sand (medium density).

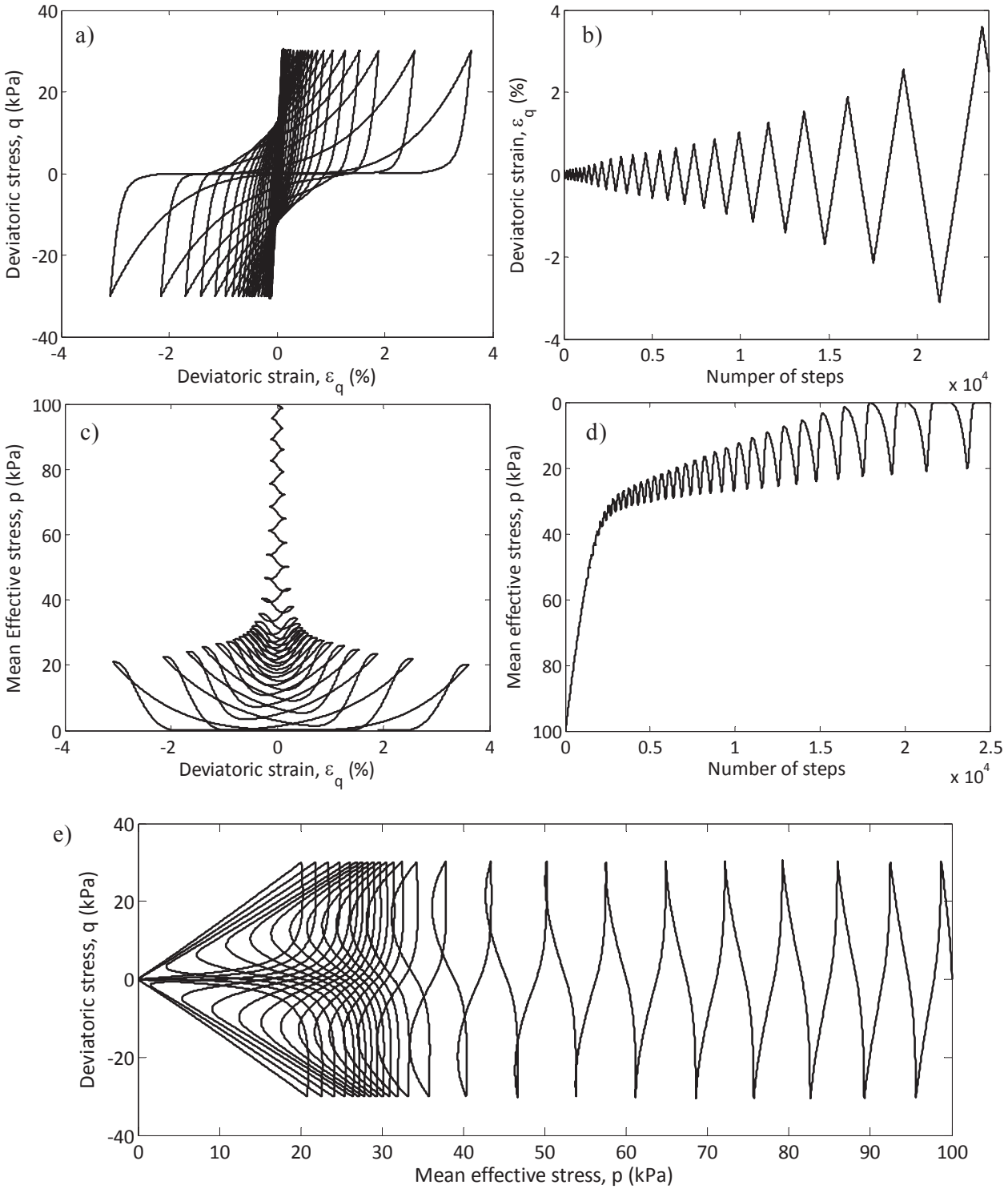

Figure 6. Simulation of cyclic undrained behavior of dense sand.

CONCLUSION

A new constitutive model for sand was briefly presented, based on modified elastoplasticity and founded on the effective stress and critical state concepts. The model, which is still under development, is an extension of the BWGG model (Gerolymos, 2002; Gerolymos and Gazetas, 2005) in 3D stress space, and combines classical elastoplasticity with a hardening law and unloading-reloding rule of the Bouc-Wen type. The predictive quality of the model was demonstrated through a series of simulations of tests in p-q space, for all combinations (4 in total) of drained and undrained loading with monotonic and cyclic loading. It was shown that it is capable of reproducing the observed behaviour without readjusting its parameters for each specific case.

AKNOWLEDGEMENTS

The financial support for this paper has been provided under the research project "DARE", which is funded through the European Research Council's (ERC) "IDEAS" Programme, in Support of Frontier Research–Advanced Grant, under contract/number ERC–2–9–AdG228254–DARE.

REFERENCES

Boulanger, R.W., Kamai R. and Ziotopoulou, K. (2011)."Numerical modeling of liquefaction effects", Proc. of 4th IASPEI/IAEE International Symposium, August 23-26, 2011, UC, Santa Barbara.

Cubrinovski, M. and Ishihara, K. (2000). "State concept and modified elastoplasticity for sand modelling", Soils and Foundations Vol. 40, No. 5, pp. 124 – 125.

Dafalias, Y. F. and Manzari, M. T. (2004). "Simple plasticity sand model accounting for fabric change effects", Journal of Engineering Mechanics, ASCE, Vol. 130, No. 6, pp. 622 – 634.

Drosos V., Gerolymos N., Gazetas G., (2012). "Constitutive model for soil amplification of ground shaking: Parameter calibration, comparisons, validation", Soil Dynamics and Earthquake Engineering (Submitted for Publication).

Gerolymos N., (2002). "Constitutive model for static and dynamic response analysis of soil, soil-pile and soil-caisson", Ph.D. thesis, National Technical University of Athens, School of Civil Engineering (in Greek).

Gerolymos N., Gazetas G. (2005), "Constitutive model for 1–D cyclic soil behavior applied to seismic analysis of layered deposits", Soils and Foundations, 45(3), 147-159.

Ishihara, K. and Towhata, I. (1980). "One-dimensional soil response analysis during earthquakes based on effective stress method", Journal of the Faculty of Engineering, University of Tokyo (B), Vol. 35, No. 4, pp. 665 – 700.

Park, S.S. and Byrne, P.M. (2004) "Practical constitutive model for soil liquefaction", Proc. of 9th Intl Sym on Numerical Mo.dels in Geomechanics NUMOG IX.

Rowe, P. W. (1962). ''The stress-dilatancy relation for static equilibrium of an assembly of particles in contact", Proc. R. Soc. London, Ser. A, 269, 500–527.

Yoshimine, M. and Ishihara, K. (1998). "Flow potential of sand during liquefaction", Soils and Foundations, Vol. 38, No. 3, pp. 189 – 198.